cannot be enlarged to describe the behavior of monomer–dimer–n-mer associations.

When applying the theory to the nonideal situations it has to be recognized that data in very dilute solutions are required. With the introduction of the Rayleigh methods and of 30-mm. double sector cells for the experiment, sufficiently greater precision in such dilute systems is promised and one is encouraged to essay such experiments. Incidentally, it is of interest that the theory developed by Steiner for *ideal* associating systems requires that the equilibrium constants be evaluated from limits taken at infinite dilution; this restriction is now relaxed.

A main objective is the determination of the quantity $L = K_2 - BM_1$. The equation of Steiner, subject to its restriction, provides it through his equation

$$\frac{\left(\frac{M_{w(c)}}{f_1 M_1} - 1\right)}{f_1 c} = \frac{4K_2}{M_1} + \frac{9K_3 f_1 c}{M_1^2} + \cdots$$

Here f_1 is the weight fraction of the monomer. It can be calculated by means of our eq. 16. Plotting the quotient against the quantity f_1c, the intercept, $4K_2/M_1$, and the limiting slope at infinite dilution, $9K_3/M_1^2$, are available. For nonideal systems undergoing the monomer–dimer association Adams and Fujita[7] already have shown that this intercept is the desired quantity $K_2 - BM_1$.

It has been proposed, for quite different purposes to be sure, that the micelles formed in solutions of paraffin-chain salts may serve as convenient models for proteins. Problems of the kind we have discussed may lead one to be able to state just how far the approach used by Debye in his study of micelle formation can be applied in protein physical chemistry. As a longer range objective it has been our purpose to indicate new means to converge on problems of this kind.

For ideal associating systems there exists another and simpler manner for testing the association mechanism instead of using eq. 14 and 14a. Using eq. 5, with all $y_i = 1$ for an ideal solution, and eq. 11 one obtains

$$(1/2AM_1r)\frac{dc}{dr} - c = K_2 c_{1a}^2 e^{2\phi_1} + 2K_3 c_{1a}^3 e^{3\phi_1} \quad (52)$$

This may be rearranged to give

$$\frac{(1/2AM_1r)\frac{dc}{dr} - c}{c_a e^{2\phi_1}} = f_{2a} + 2f_{3a}e^{\phi_1} \quad (53)$$

A plot of the quantity on the left-hand side of eq. 53 against e^{ϕ_1} gives a horizontal line for a monomer–dimer association and an inclined line for a monomer–dimer–trimer or monomer–trimer association. We can distinguish between a monomer–dimer–trimer and a monomer–trimer association with a second plot; we note that

$$\frac{3c - (1/2AM_1r)dc/dr}{c_a e^{\phi_1}} = 2f_{1a} + f_{2a}e^{\phi_1} \quad (54)$$

Here a plot of the left-hand term of eq. 54 against e^{ϕ_1} gives a horizontal line for a monomer–trimer association and an inclined straight line for a monomer–dimer or monomer–dimer–trimer association.

Acknowledgment.—We wish to thank Drs. J. H. Elliott, F. E. LaBar, D. L. Filmer, and V. J. MacCosham for their comments and interest in this work.

[CONTRIBUTION FROM THE DEPARTMENT OF CHEMISTRY, WILLIAM MARSH RICE UNIVERSITY, HOUSTON, TEXAS, AND THE DEPARTMENT OF PHYSICS, TULANE UNIVERSITY, NEW ORLEANS, LOUISIANA]

Morphology of Colloidal Gold—A Comparative Study

BY W. O. MILLIGAN[1a] AND R. H. MORRISS[1b]

RECEIVED MARCH 2, 1964

A comparative study of the morphology of colloidal gold was made using light absorption and scattering, X-ray diffraction line broadening, and electron microscopy. A series of colloidal gold samples ranging in average particle "diameter" from 10 to 400 Å. and exhibiting a wide range of crystallite morphology was prepared and examined by each method. Extinction coefficients, absolute light scattering coefficients, and depolarization factors were measured for wave lengths between 4000 and 6500 Å. Using the theory of Mie for the interaction of light with conducting spheres and the extension of this theory by Gans to ellipsoids of various axial ratios, the approximate shape of the crystallites was calculated. The pure diffraction line broadening of the (200), (111), (220), and (311) reflections was measured, and by applying the Scherrer equation, the mean crystallite dimension along [100], [111], [110], and [311] was calculated. The morphology as calculated from light absorption and scattering and X-ray diffraction was found to be in fairly close agreement with the electron microscopic findings for most colloidal gold samples. However, each technique, including electron microscopy, was found to have limitations, in particular particle size ranges.

I. Introduction

Beginning with the slit ultramicroscope which was developed shortly after 1900, several indirect methods have been employed to study the morphology of colloidal particles. One method is that of light absorption and scattering. In 1908 Mie[2a] presented a theoretical treatment of the interaction of light with small, conducting spheres. On the basis of Maxwell's electromagnetic theory, Mie calculated the true absorption and the intensity and polarization properties of light scattered by spherical particles of varying size in terms of the macroscopic optical properties of the metal. In 1912 Gans[2b] extended the calculations of Mie by generalizing the particle shape to prolate and oblate ellipsoids of revolution. Whereas Mie's cal-

(1) (a) Department of Chemistry, William Marsh Rice University; present address Texas Christian University, Fort Worth, Texas; (b) Department of Physics, Tulane University.

(2) (a) G. Mie, *Ann. Physik*, **25**, 377 (1908); (b) R. Gans, *ibid.*, **37**, 833 (1912).

culations apply to particles smaller than the wave length of light, Gans' calculations are limited to particles smaller than approximately one-tenth the wave length of light.

In 1928 Lange[3] made a detailed investigation of the absorption and scattering of light by gold hydrosols over the wave length range 4250–7000 Å. The absorption measurements were in good agreement with Mie's theory indicating the particles to be approximately spherical in shape. However, the data obtained for the degree of polarization of the transversely scattered light were in better agreement with Gans' theory, thereby indicating ellipsoidal morphology. To explain this seeming contradiction, Lange postulated that a large majority of particles in a gold hydrosol are spherical in shape which manifest themselves in absorption measurements, and a lesser number of particles which are in the form of ellipsoids of revolution account for the polarization properties of the scattered light. In 1937 Krishnan[4] measured the absorption and polarization of a group of gold hydrosols over the wave length range 3000–7000 Å. From both sets of data, he found the particles to behave optically as prolate ellipsoids with an axial ratio of 0.75. Sivarajan[5] measured the scattering intensities for a group of gold hydrosols similar to those of Krishnan and likewise obtained good agreement with Gans' theory for prolate ellipsoids of axial ratio 0.75.

Scherrer[6] in 1918 showed that the mean dimension, D, of the crystallites composing a crystalline powder is related to the pure diffraction line broadening, β, by the equation

$$D = \frac{K\lambda}{\beta \cos \theta} \qquad (1)$$

where K is a constant factor which is related to the shape of the crystallites and the manner in which D and β are defined. If D is referred to as D_{hkl} and is the effective crystallite thickness in a direction perpendicular to the (hkl) planes and $\beta = \beta_{1/2}$ is defined as the half-maximum line breadth, it has been shown[6,7] that K has a value of approximately 0.9 and is independent of the crystal shape. The Scherrer equation then becomes

$$D_{hkl} = \frac{0.9\lambda}{\beta_{1/2} \cos \theta} \qquad (2)$$

By measuring several values of $\beta_{1/2}$ corresponding to different (hkl) reflections, one can obtain some indication of the crystal shape characteristics. In 1938 Jones[8] carried out an X-ray diffraction line broadening experiment on a sample of colloidal gold and found the average dimensions of the particles to be 703 × 176 × 176 Å. which would indicate the particles to be rod shaped.

The development of the electron microscope in the late 1930's offered a new, direct means of studying the morphology of colloidal particles. Beischer and Krause[9] were the first to examine colloidal gold in the electron microscope and found a Gaussian distribution of particles in the form of octahedrons. Turkevich, Stevenson, and Hillier[10] made an extensive electron microscopic study of gold hydrosols prepared by several standard methods and found the size distribution and morphology to vary with the method of preparation. More recently, Morriss and Milligan[11] concluded from a high resolution electron microscopic examination of colloidal gold that the most common crystallite form is the cuboctahedron, in which {111} faces are more developed than are {100} faces. This cuboctahedral shape accounts for the fact that colloidal gold particles often appear to be spherical in the electron microscope, especially when examined at relatively low magnification.

In 1954 Turkevich, Garton, and Stevenson[12] combined an electron microscopic examination with a study of the absorption spectra of a series of gold sols of various particle size and shape. The extinction coefficient curves obtained for most sols were in fair agreement with the theoretical values of Mie for spherical particles. However, a gold sol produced using acetylene as the reducing agent gave an absorption spectrum showing two absorption maxima. They suggested that the maximum at 5250 Å. was due to the majority of spherical particles present in the sol, whereas the maximum at 6750 Å. was due to one-third of the particles in the form of platelets of trigonal symmetry.

With the exception of this work of Turkevich, Garton, and Stevenson, the other studies concerning the morphology of colloidal gold have been carried out using a single technique, *i.e.*, either slit ultramicroscopy, light absorption and scattering, X-ray diffraction line broadening, or electron microscopy. It was the purpose of this present investigation to examine the morphology of a large series of colloidal gold samples using each of these methods with the exception of slit ultramicroscopy. The accuracy of the indirect techniques has been compared to that of the direct method of electron microscopy.

II. Experimental

Preparation of Samples.—Colloidal gold was chosen for this investigation since the morphology of the particles can be varied by slight changes in the method of preparation. In addition, gold hydrosols containing particles covering the entire colloidal size range of 10–10,000 Å. may readily be prepared. The method of preparation consisted of the reduction of a chloroauric acid solution with one of the following reducing agents: sodium citrate, hydrogen peroxide, hydroxylamine hydrochloride, citric acid, and phosphorus in ether. Changes in particle size and shape were affected by variations in the type of reducing agent, concentration of reagents, and pH value of reagents. In general, it was found that lowering the pH value caused the {111} faces to develop at the expense of the {100} faces, the extreme case producing very thin platelets of trigonal symmetry, designated by Suito[13] as "trigons."

Light Absorption and Scattering.—Extinction coefficients for wave lengths 4200 Å. through 6500 Å. were measured using a Cary recording spectrophotometer. The light scattering measurements were made with a Phoenix-Brice light scattering photometer. The photometer consists essentially of a monochromatic

(3) B. Lange, *Z. physik. Chem.*, **132**, 1 (1928).
(4) R. S. Krishnan, *Proc. Indian Acad. Sci.*, **5**, 94 (1937).
(5) S. R. Sivarajan, *ibid.*, **37**, 418 (1953).
(6) P. Scherrer, *Nachr. kgl. Ges. Wiss. Göttingen*, **2**, 98 (1918).
(7) L. Bragg, "The Crystalline State, A General Survey," Vol. 1, G. Bell and Sons, Ltd., London, 1949, p. 189.
(8) F. W. Jones, *Proc. Roy. Soc.* (London), **A166**, 16 (1938).
(9) D. Beischer and F. Krause, *Naturwissenschaften*, **25**, 825 (1937).
(10) J. Turkevich, P. C. Stevenson, and J. Hillier, *Discussions Faraday Soc.*, **11**, 55 (1951).
(11) R. H. Morriss and W. O. Milligan, *J. Electronmicroscopy* (Tokyo), **8**, 17 (1960).
(12) J. Turkevich, G. Garton, and P. C. Stevenson, *J. Colloid Sci., Suppl.*, **1**, 26 (1954).
(13) E. Suito and N. Ueda, *J. Electronmicroscopy* (Tokyo), **1**, 33 (1953).

incident beam of radiation, a six-sided scattering cell for measurements at 0, 45, 90, and 135°, a photomultiplier tube and galvanometer, a standard opal glass diffusor, and removable polarizer and analyzer. Inasmuch as the solutions were prepared from extremely dust-free distilled water, it was neither necessary or desirable to filter the sols prior to examination in the light scattering apparatus. Monochromatic filters were used to isolate wave lengths of 3650, 4060, 4360, 5460, and 5780 Å. from a high pressure Type AH-3 mercury lamp. The light scattering photometer was used to measure the depolarization factor, ρ_u, and absolute light scattering coefficient.

The depolarization factor, ρ_u, is a measure of the degree of polarization of the light scattered in the transverse horizontal direction when the incident beam is unpolarized. The depolarization factor is determined by inserting the analyzer, setting the receiver at 90°, reading the galvanometer deflection, H_u, with the analyzer set to pass horizontal electric vector vibrations, and the deflection, V_u, with the analyzer set for vertical vibrations. The depolarization factor, ρ_u, is then equal to the ratio of H_u to V_u.

The Phoenix–Brice light scattering photometer is also designed for the measurement of absolute light scattering coefficients. The light scattering coefficient K_s, is identical with the turbidity, τ, of a solution, which is defined by

$$P = P_0 \exp(-\tau x) \qquad (3)$$

where P and P_0 are the total scattered and incident radiant flux, respectively, and x is the distance the incident radiation passes through the solution. Brice[14,15] has developed a relationship for the turbidity in terms of a ratio of galvanometer deflections for the 90° scattering and for the primary beam (0°) reduced in intensity by neutral filters and diffused by an opal glass plate. Turbidity measurements were made at wave lengths of 4360 and 5460 Å.

X-Ray Diffraction Line Broadening.—The accuracy which can be attained with the Scherrer equation is limited by the preciseness with which the pure diffraction line broadening, $\beta_{1/2}$, can be determined. Although the pure diffraction broadening is best differentiated from the instrumental broadening, b, by use of Fourier transform theory, Warren[16] showed that when β and b are both Gaussian curves the breadths have the relationship

$$B^2 = \beta^2 + b^2 \qquad (4)$$

where B is the observed line breadth. Although these conditions are never exactly satisfied in practice, the use of eq. 4 simplifies the calculations considerably and in recent years has been widely used for correcting Debye–Scherrer line widths. Considerable uncertainty may result when this method is used to calculate absolute crystallite size; however, in the present experiments the crystallite shape was of primary interest.

Using a Philips X-ray power supply, Debye–Scherrer patterns were obtained using a Buerger-type camera. The gold hydrosols were first evaporated in a vacuum desiccator until only a powder or thin coating of gold was left in the container. The resulting powder was then placed in a thin-walled Lindemann glass capillary tube 0.3 mm. in diameter. In order to eliminate as much instrumental line broadening as possible, it was necessary to modify the beam collimator on the Buerger camera. The first aperture of the collimator, consisting of a relatively large rectangular slit, was covered with a thin sheet of lead into which an accurately centered hole was drilled with a number 80 (0.343-mm.) drill. Copper radiation filtered by nickel foil was used, the measurements being made on unresolved Kα lines. Because of variations in development and film sensitivity, it was necessary to prepare intensity scale strips maintaining constant exposure times so that valid comparisons could be made between different patterns.

Each diffraction pattern, with its intensity scale strip, was examined in a Leeds and Northrup recording microphotometer. After subtracting the background intensity, the width of the diffraction peak at half maximum intensity was measured for the first four lines of each pattern, corresponding to the (111), (200), (220), and (311) reflections. To compensate for film shrinkage and a possible variation in scanning or recorded speeds, a correction factor was determined by calculating the theoretical positions of the diffraction peaks and comparing them with the observed peaks. Since for Debye–Scherrer techniques of ordinary precision the pure diffraction line broadening is negligible for crystallites over 1000 Å. in "diameter," the instrumental line broadening, b, was measured using a gold sample containing particles over 1000 Å. After measuring the observed broadening, B, for each sample and the instrumental broadening, b, which was a constant for this particular experimental set-up, the pure diffraction broadening, β, was calculated using eq. 4. The effective thickness, D_{hkl}, of the crystallites was then calculated using eq. 2.

(14) B. A. Brice, M. Halwer, and R. Speiser, *J. Opt. Soc. Am.*, **40**, 768 (1950).

(15) B. A. Brice, G. C. Nutting, and M. Halwer, *J. Am. Chem. Soc.*, **75**, 824 (1953).

(16) B. E. Warren, *J. Appl. Phys.*, **12**, 375 (1941).

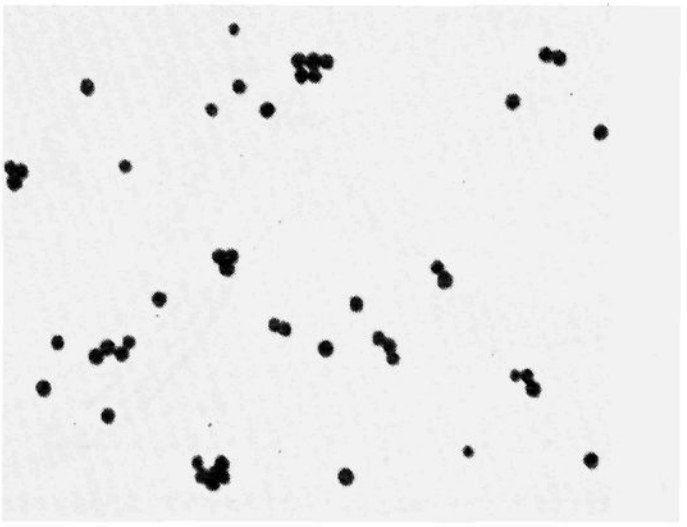

Fig. 1.—Electron micrograph of gold hydrosol, S-1 (sodium citrate). Magnification: 80,000 diameters, 1 mm. = 125 Å.

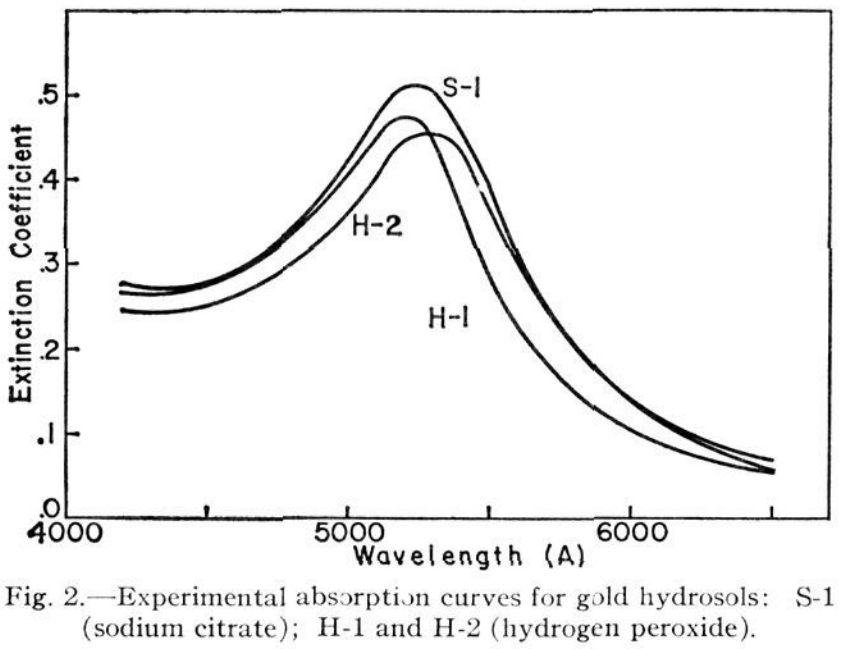

Fig. 2.—Experimental absorption curves for gold hydrosols: S-1 (sodium citrate); H-1 and H-2 (hydrogen peroxide).

Electron Microscopy.—The gold hydrosols were examined with both Philips type EM-100 and EM-100B electron microscopes. A small drop of the hydrosol was allowed to evaporate on a thin carbon membrane mounted on a copper grid and then examined in the electron microscope by standard methods.

III. Results and Discussion

Sodium Citrate.—The reduction of chlorauric acid with sodium citrate produces an unusually uniform gold hydrosol, both with respect to particle shape and size. This can be observed in the electron micrograph of sol S-1 shown in Fig. 1. By direct measurement from electron micrographs of 1000 particles, the average particle size was calculated to be 176 Å. with a small standard deviation of 5 Å. The particles appear to be approximately spherical in the electron micrograph. The extinction coefficients of sol S-1 are shown in Fig. 2 and are in close agreement with the theoretical results of Mie (Fig. 3) for conducting spheres of a 200 Å. diameter. The observed depolarization factors, ρ_u, for sol S-1 are shown in Fig. 4. From the theoretical values for ρ_u as tabulated in Table I, it is evident that the ρ_u-values approach zero as the axial ratio approaches a value of 1.000, corresponding to a spheri-

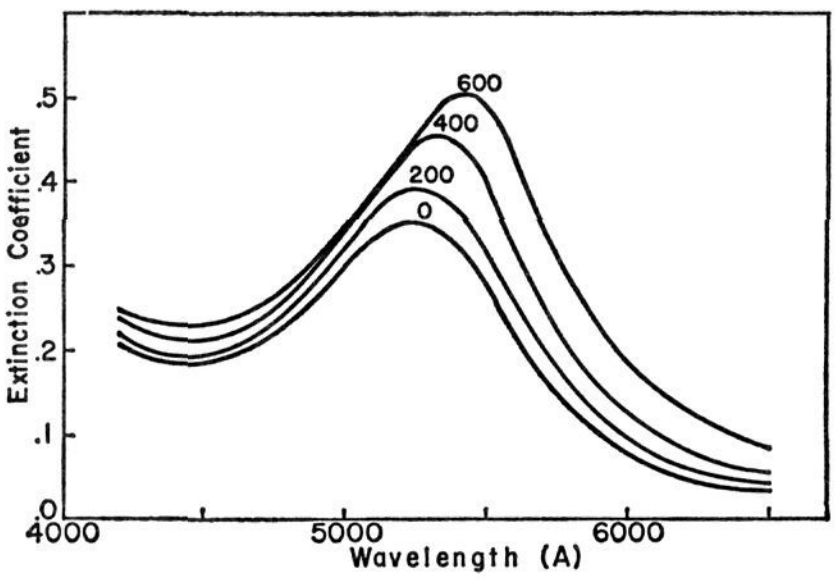

Fig. 3.—Mie's theoretical curves for spherical particles of diameters 0, 200, 400, and 600 Å.

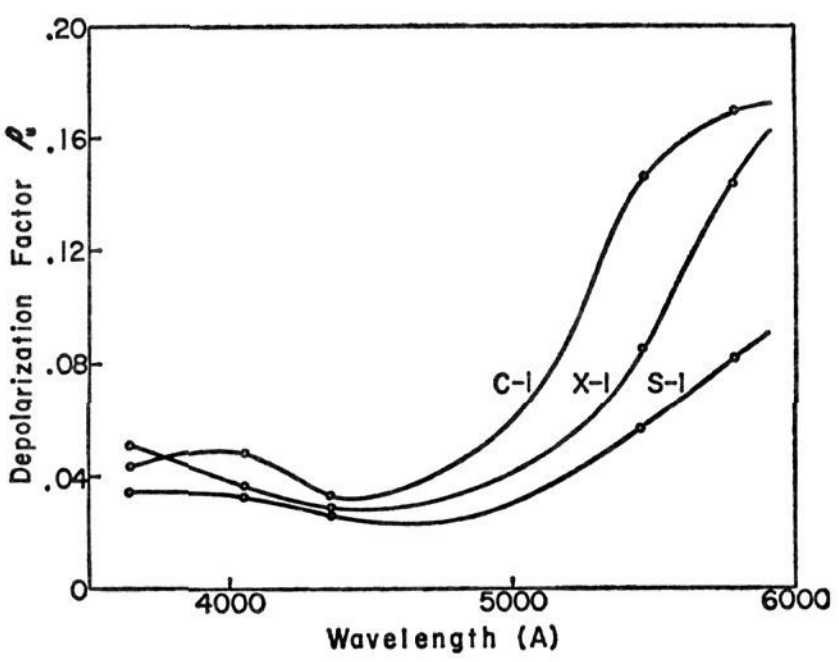

Fig. 4.—Depolarization of scattered light for gold hydrosols: C-1 (citric acid); X-1 (hydroxylamine hydrochloride); S-1 (sodium citrate).

cal shape. The values of ρ_u for sol S-1 are relatively small, indicating that the particles are approximately spherical.

TABLE I

GANS' THEORETICAL VALUES OF DEPOLARIZATION FACTOR ρ_u

Wave length, Å.	Prolate ellipsoid, Axial ratio 0.00	0.58	0.82	Sphere 1.00	Oblate ellipsoid, Axial ratio 1.28	2.63	6.25	0.00
4200	0.358	0.047	0.005	0.000	0.088	0.093	0.205	0.306
4500	.379	.044	.005	.000	.009	.094	.205	.305
5000	.766	.323	.015	.000	.021	.191	.361	.191
5250	.403	.282	.031	.000	.035	.263	.442	.559
5500	.478	.518	.046	.000	.024	.281	.379	.561
6000	*.874*	*.171*	*.020*	*.000*	*.018*	*.065*	*.374*	*.481*
6500	.022	.105	.012	.000	.010	.056	.320	.416

The D_{hkl} values along [111], [100], [110], and [311] as obtained from X-ray diffraction line broadening are listed in Table II. The dimension along the four directions are in close agreement, again indicating a spherical shape. The four sets of data for sol S-1 show exceptionally close agreement in predicting the crystallites to deviate only slightly from a spherical shape. One can conclude from this that the particles are in the form of cube-octahedrons with the {100} and {111} faces equally developed. This is in accord with the Kossel–Stranski theory of crystal growth.

Hydrogen Peroxide.—Sols H-1 and H-2 were prepared using hydrogen peroxide as the reducing agent

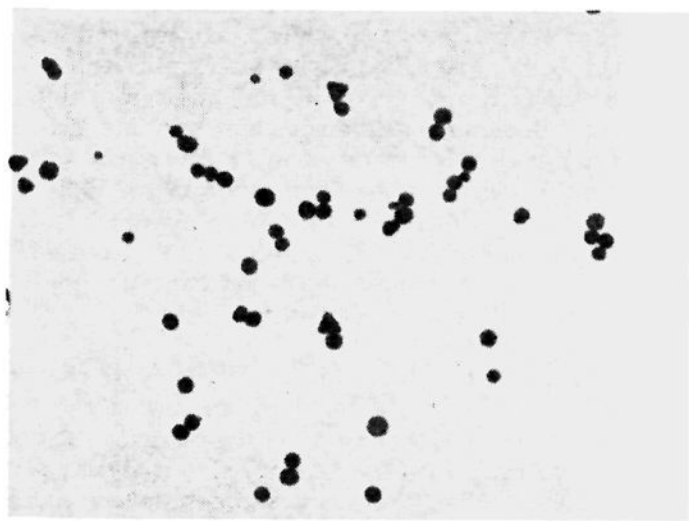

Fig. 5.—Electron micrograph of gold hydrosol, H-2 (hydrogen peroxide). Magnification: 80,000 diameters, 1 mm. = 125 Å.

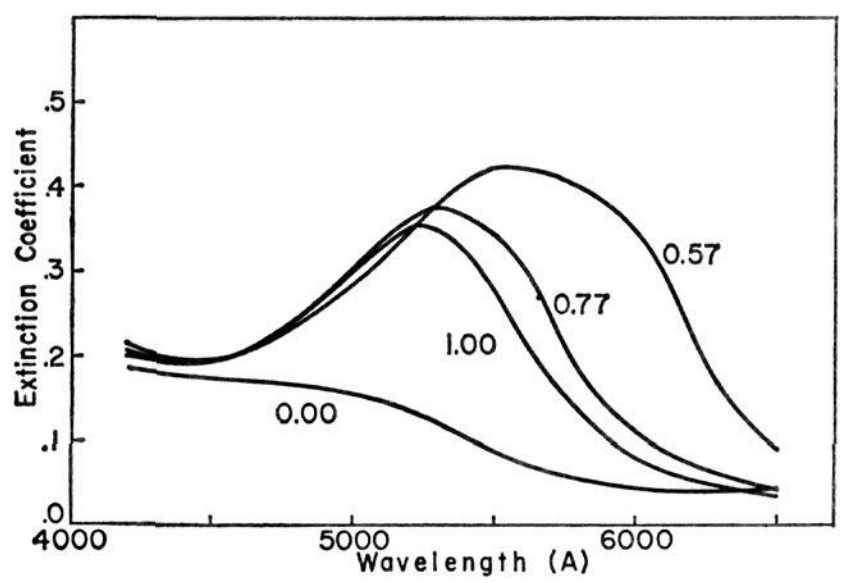

Fig. 6.—Gans' theoretical curves for prolate ellipsoids of axial ratios 0.00, 0.57, 0.77, and 1.00.

TABLE II

X-RAY DIFFRACTION LINE BROADENING

Sol no.	D_{111}, Å.	D_{200}, Å.	$D_{?\cdot 0}$, Å.	D_{311}, Å.	D_{av}, Å.
S-1	174	172	179	175	175
H-1	165	147	146	148	151
H-2	123	136	210	279	187
X-1	421	259	250	580	378
M-1	98	73	88	101	90
M-2	99	94	97	104	98
M-3	136	122	129	137	131
P-1	162	101	136	157	139
P-2	251	192	199	198	210
P-3	302	304	271	308	296
P-4	363	408	332	373	369

under identical conditions with the exception of the pH value of the distilled water. The pH value of the water was lowered from 4.8 to 4.1 in preparing sol H-2. From electron microscopy the particles of sol H-1 appear very similar to those of S-1, *i.e.*, spherical in shape and uniform in size. From Fig. 5 it can be seen that H-2 contains a few thin platelets of trigonal symmetry, in addition to "spherical" particles which appear to be in the majority. The presence of "trigons" in sol H-2 are apparent in the absorption data as shown in Fig. 2. The extinction coefficient peak for H-2 is slightly broadened and shifted to the longer wave length region. From the theoretical curves for prolate ellipsoids shown in Fig. 6, it is seen that a deviation from sphericity causes broadening and a shift to longer wave lengths. Depolarization factors, ρ_u, for H-1 and H-2 are shown in Fig. 7. The value of

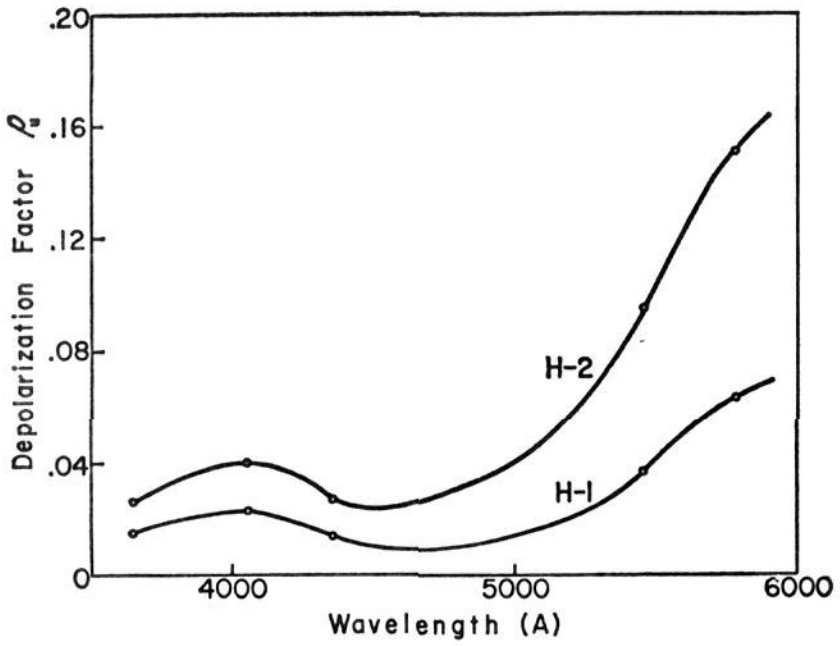

Fig. 7.—Depolarization of scattered light for gold hydrosols: H-1 and H-2 (hydrogen peroxide).

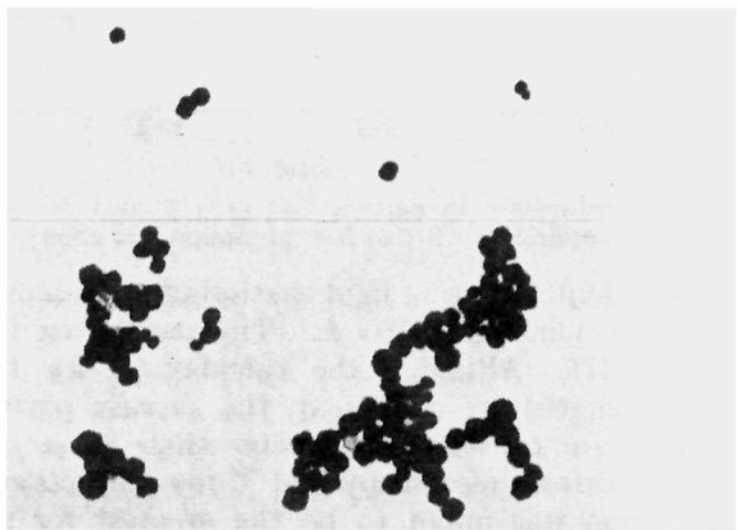

Fig. 8.—Electron micrographs of two areas of gold hydrosol: X-1 (hydroxylamine hydrochloride). Magnification: 80,000 diameters, 1 mm. = 125 Å.

ρ_u for H-2 is approximately twice that of H-1 for each of the five wave lengths at which measurements were made. This indicates the presence of "nonspherical" particles in sol H-2. Each curve shows a maximum around 4000 Å. and a sharp rise in the longer wave length region, starting at approximately 5250 Å. The theoretical values of ρ_u as a function of wave length for a prolate ellipsoid of axial ratio 0.82 (Table I) show the same general type of behavior; however, the theoretical values are considerably higher in magnitude than are the observed values of sol H-2. The observed values appear to be approximately midway between the theoretical values for a sphere and a prolate ellipsoid of axial ratio 0.82.

The X-ray diffraction D_{hkl} values for H-1 are extremely uniform, with the exception of D_{111} which is slightly larger. This result suggests that the average crystallite form is the cuboctahedron, with the possibility of the $\{100\}$ faces being developed slightly more than the $\{111\}$ faces. The "trigons" in sol H-2 show their presence in the line broadening results, the wide range of D_{hkl} values indicating a considerable deviation from sphericity. The relatively small value obtained for D_{111} indicates a small dimension along [111]. This implies that the large faces of the thin platelets corresponds to (111) faces. This is in agreement with results on "trigons" obtained by Suito and Ueda[13] using electron diffraction techniques.

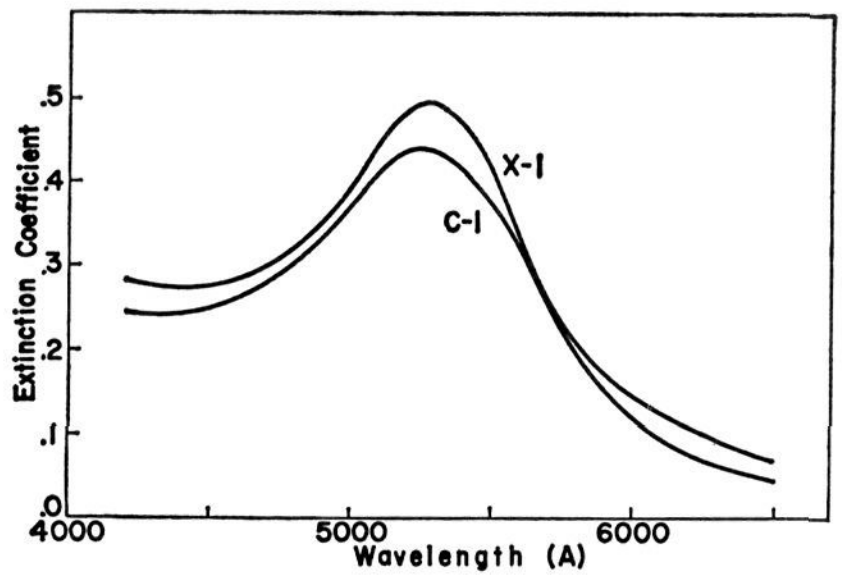

Fig. 9.—Experimental absorption curves for gold hydrosols: C-1 (citric acid); X-1 (hydroxylamine hydrochloride).

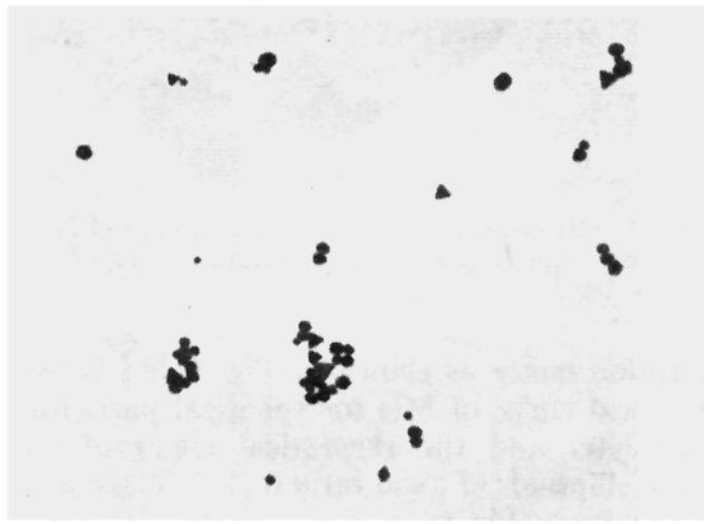

Fig. 10.—Electron micrograph of gold hydrosol, C-1 (citric acid). Magnification: 80,000 diameters, 1 mm. = 125 Å.

Hydroxylamine Hydrochloride.—An electron micrograph of sol X-1 prepared using hydroxylamine hydrochloride as the reducing agent is shown in Fig. 8. A large number of particles appear to be "cubical" in form, indicating that the $\{100\}$ faces are more fully developed than are the $\{111\}$ faces. This is in agreement with D_{hkl} values obtained from line broadening measurements in which the D_{hkl} values along [111] and [311] were found to be considerably greater than those along [100] and [110]. The average D_{hkl} value of 378 Å. is considerably larger than 228 Å., the average particle size obtained from electron microscopy. This is due primarily to the wide distribution of particle size found in sol X-1. The larger particles contribute more strongly to the over-all intensity, whereas the small particles produce broader diffraction maxima which tend to merge into the background. Throughout these experiments, the disagreement between the average particle size as measured from X-ray diffraction and electron microscopy was found to be proportional to the particle size distribution. The absorption curve for X-1 is shown in Fig. 9 and is in close agreement with the theoretical predictions of Mie for spherical particles. Relatively large values of the depolarization factor, ρ_u, were observed for X-1 (Fig. 4). This is primarily due to the large size of the particles rather than shape anisotropy.

Citric Acid.—Sol C-1 prepared using citric acid as the reducing agent contains an extremely large number of "trigons," as observed in the electron micrograph (Fig. 10). Some larger "trigons" are shown in Fig. 11. The

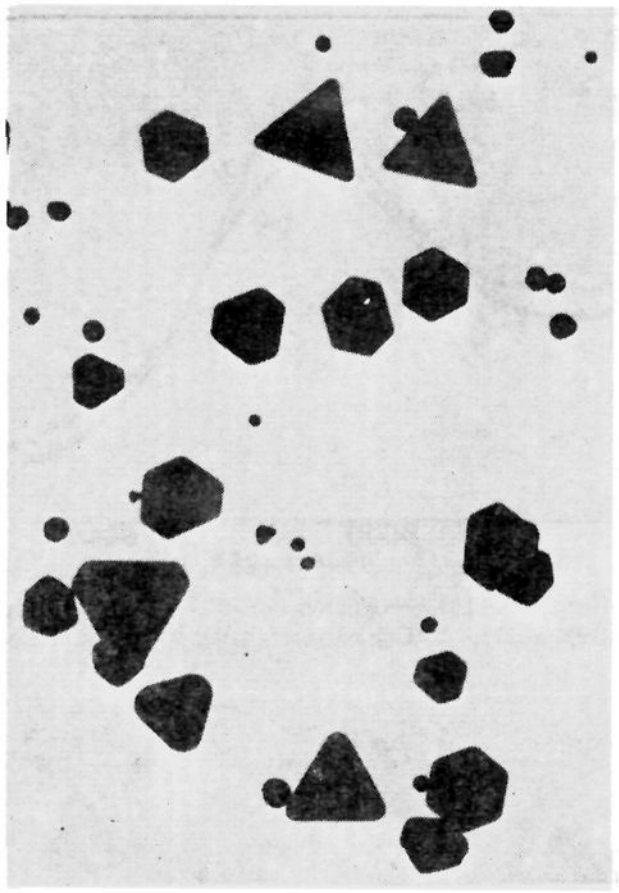

Fig. 11.—Electron micrograph of gold hydrosol (citric acid), illustrating large "trigons." Magnification: 40,000 diameters, 1 mm. = 250 Å.

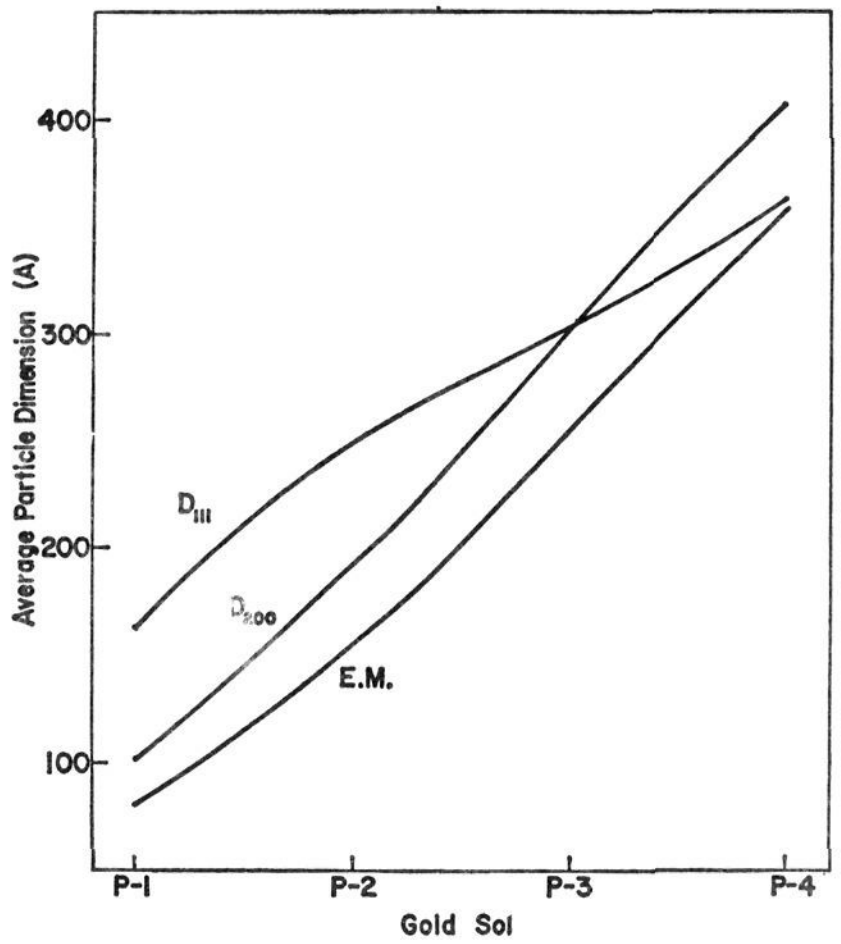

Fig. 12.—Increase in particle size of a graded series of gold hydrosols: P-1 to P-4 (phosphorus in ether).

absorption curve as shown in Fig. 9 lies between the theoretical curve of Mie for spherical particles 200 Å. in diameter and the theoretical curve of Gans for prolate ellipsoids of axial ratio 0.77. Shape anisotropy is also observable from the ρ_u values shown in Fig. 4. The depolarization factors for sol C-1 were found to be larger than for any sol in the series. X-Ray diffraction data were not obtained for C-1.

Carbon Monoxide.—A series of sols, M-1, M-2, and M-3, were prepared using carbon monoxide as the reducing agent. The D_{hkl} values obtained from X-ray diffraction are fairly uniform for each of the three sols, indicating the particles to be approximately spherical. The agreement between the average particle size as obtained from x-ray diffraction and electron microscopy improves as the average particle size increases.

Phosphorus.—The P series of gold sols was prepared by the nuclear method. Sol P-1 was prepared using phosphorus in ether as the reducing agent and served as the nuclear sol. Sols P-2, P-3, and P-4 were then prepared by subsequent growth of the nuclei using hydroxylamine hydrochloride as the growth medium. In Fig. 12 is shown the rates with which the D_{111} and D_{100} values increased along with the rate with which the electron microscopic average particle size increased. From the X-ray diffraction results, it is seen that the growth along [111] progressed at a lower rate than along [100]. This suggests that although the nuclear particles (P-1) tended toward a cubical shape, subsequent growth progressed more rapidly along [100], thus causing the {111} faces to develop at the expense of the {100} faces. The external form of the particles in sol P-4, therefore, tended to be octahedral.

Absolute Light Scattering Coefficients.—Although relative values of light scattering coefficients for gold sols have been reported by others, absolute values have not been previously measured. Applying Mie's theory for small, spherical particles average particle diameters were calculated using light scattering coefficients measured at 4360 and 5460 Å. The results are listed in Table III. Although the calculations for the two wave lengths are consistent, the average particle size values are considerably greater than those obtained from electron microscopy and X-ray diffraction. This deviation was found to be the greatest for sol C-1, which contained the largest percentage of "non-spherical" particles.

TABLE III

AVERAGE PARTICLE SIZE

	—Light scattering—			—Electron microscopy—	
Sol. no.	4360 Å.	5460 Å.	X-Ray diffraction line broadening, Å.	Average size, Å.	Standard deviation, Å.
S-1	291	286	175	176	6
H-1	253	231	151	157	11
H-2	310	313	187	197	26
X-1	...	...	378	228	42
C-1	235	228	...	125	6
M-1	91	74	90	50	5
M-2	153	153	98	75	4
M-3	189	183	131	122	5
P-1	...	...	139	81	5
P-2	...	...	210	155	17
P-3	...	...	296	256	26
P-4	...	...	369	358	97

IV. Summary

From electron microscopy the gold sols were found to be characterized by crystallites of three basic shapes: "spherical," or "cuboctahedral," in which both the {111} and the {100} faces are developed, the {111} faces to a greater extent; "cubical," in which the {100} faces on the crystal habit are predominant; and "trigonal," in which the morphology is that of thin platelets of trigonal symmetry. In morphological determinations of colloidal gold the electron microscope is limited to particles larger than approximately 100 Å. This is particularly true in the case of a cuboctahedral

particle resting on a (111) face which gives rise to a dodecahedral projection. A resolution of the order of 5 Å. would be required to resolve the edges of a 12-sided projection of a 100 Å. particle.

The calculated values for the extinction coefficients between 4000 and 6500 Å. were in very close agreement with the theoretical values of Mie for conducting spheres. This agreement was particularly good for sols containing predominantly cuboctahedral particles. The presence of "cubical" or "trigonal" particles broadened the absorption peak slightly and shifted it to the higher wave length region. The measured extinction coefficients were then in closer agreement with the theoretical values of Gans for prolate ellipsoids of an axial ratio of 0.90. This is in agreement with the results of Krishnan,[4] who from absorption measurements found colloidal gold particles to behave optically as prolate ellipsoids with an axial ratio of 0.75. It is somewhat surprising that gold sols containing platelets of trigonal symmetry should behave as prolate or elongated ellipsoids rather than oblate or flattened ellipsoids of revolution. However, from Fig. 13 it is observed that the effect of flattening is also to broaden the peak and shift it to a higher wave length. A more rigorous treatment of the absorption data might show closer agreement with the results of Gans for oblate ellipsoids of revolution. The double absorption peak reported by Turkevich, Garton, and Stevenson[12] was not observed in this study for any of the gold sols containing "trigons."

The depolarization coefficients, ρ_u, for sols containing "trigons" were found to have approximately twice the value as sols containing predominantly "spherical" and "cubical" particles. The ρ_u curves showed a maximum around 4000 Å. and a sharp rise in the longer wave length region, beginning at approximately 5250 Å. Shape anisotropy can easily be detected for particles in the 10–100 Å. range from measurements of ρ_u. Therefore, light scattering measurements provide a good supplement to electron microscopy when the morphology of extremely small particles is of interest.

The absolute light scattering coefficient measurements consistently gave high values for the average particle size. The best results were obtained for sols containing "spherical" particles. In addition to particle size, light scattering intensity is greatly dependent on particle shape.

The three crystal habits were easily discernible from the D_{hkl} values obtained from X-ray diffraction line broadening measurements. Average particle size values were in fair agreement with electron microscopic results, the best agreement being found for sols containing uniform particles of approximately 150 Å. in "diameter." Measurements on a series of sols prepared using the nuclear method gave indication that, although the nuclear particles were "cubical" in shape, the subsequent growth progressed at a more rapid rate along [100] than along [111]. As is the case with ρ_u measurements, X-ray diffraction line broadening can be applied in the morphological study of particles in the 10–100 Å. range, although best results are obtained for particles in the 100–200 Å. range.

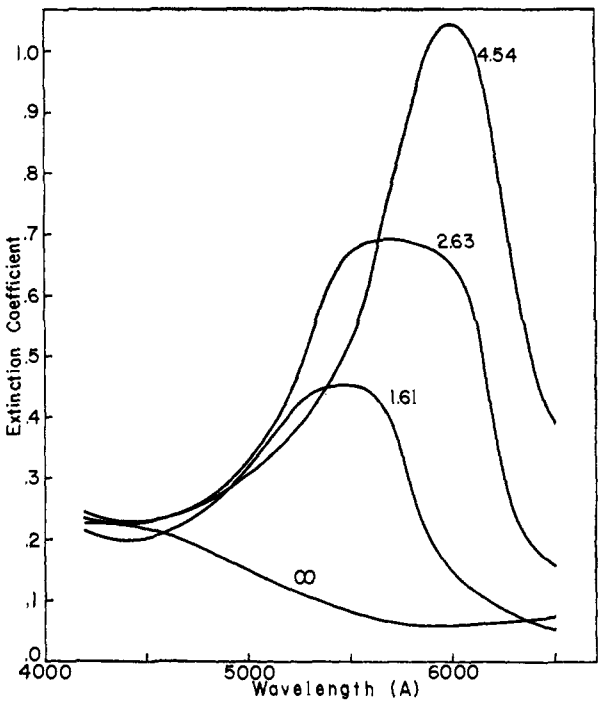

Fig. 13.—Gans' theoretical curves for oblate ellipsoids of axial ratios ∞, 1.61, 2.63, and 4.54.

Acknowledgment.—We acknowledge with thanks the kindness of Humble Oil and Refining Co. in allowing us to use their light scattering photometer, as well as providing R. H. M. with a predoctoral fellowship. We are grateful to the M. D. Anderson Foundation for providing a postdoctoral fellowship for R. H. M. We wish to thank Mr. R. C. Hoy for performing the X-ray diffraction measurements. This study was sponsored in part by the National Science Foundation. We acknowledge numerous helpful discussions with Dr. P. J. W. Debye.